

Effect of charge-transfer complex on the energy level alignment between graphene and organic molecules

Giyeol Bae, Hyun Jung, Noejung Park, Jinwoo Park, Suklyun Hong et al.

Citation: *Appl. Phys. Lett.* **100**, 183102 (2012); doi: 10.1063/1.4709428

View online: <http://dx.doi.org/10.1063/1.4709428>

View Table of Contents: <http://apl.aip.org/resource/1/APPLAB/v100/i18>

Published by the AIP Publishing LLC.

Additional information on *Appl. Phys. Lett.*

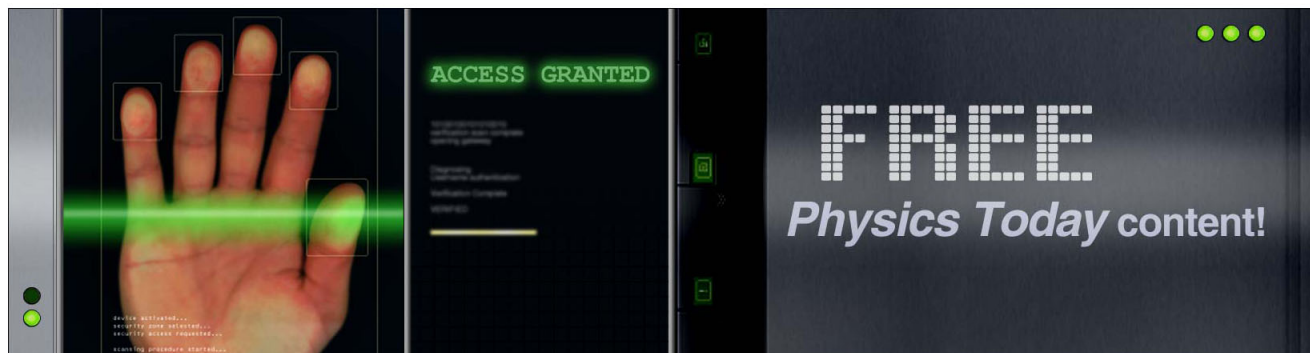
Journal Homepage: <http://apl.aip.org/>

Journal Information: http://apl.aip.org/about/about_the_journal

Top downloads: http://apl.aip.org/features/most_downloaded

Information for Authors: <http://apl.aip.org/authors>

ADVERTISEMENT



Effect of charge-transfer complex on the energy level alignment between graphene and organic molecules

Giyeol Bae,¹ Hyun Jung,² Noejung Park,^{2,a)} Jinwoo Park,³ Suklyun Hong,³ and Wanjun Park¹

¹Division of Nanoscale Semiconductor Engineering, Hanyang University, Seoul 133-791, South Korea

²Interdisciplinary School of Green Energy and Low Dimensional Carbon Materials Center, Ulsan National Institute of Science and Technology (UNIST), Ulsan 689-798, Korea

³Department of Physics and Graphene Research Institute, Sejong University, Seoul 143-747, South Korea

(Received 11 February 2012; accepted 16 April 2012; published online 1 May 2012)

We performed density-functional theory calculations to study the electronic structures at the interfaces between graphene and organic molecules that have been used in organic light-emitting diodes. In terms of work function, graphene itself is not favorable as either anode or cathode for commonly used electron or hole transport molecular species. However, the formation of charge transfer complex on the chemically inert sp^2 carbon surface can provide a particular advantage. Unlike metal surfaces, the graphene surface remains non-bonded to electron-accepting molecules even after electron transfer, inducing an improved Fermi-level alignment with the highest-occupied-molecular-orbital level of the hole-injecting-layer molecules. © 2012 American Institute of Physics. [<http://dx.doi.org/10.1063/1.4709428>]

Graphene, a two-dimensional monolayer of sp^2 -bonded carbons, has inspired a wide variety of research activities, from practical materials engineering to pure scientific studies of electron gas in low dimensions.^{1–4} Many potential applications have been suggested, including composite material,^{5,6} energy storage,⁷ and high-speed semiconductors.^{8,9} Among them, the feasibility of graphene as a transparent electrode is particularly intriguing.^{10–12} Transparent electrodes are key components in modern flat panel displays, conductive films used in touch screens, and photovoltaic devices such as solar cells. Indium-tin-oxide (ITO) is the most widely used material for transparent conductors. However, the scarcity of indium resources necessitates an urgent search for alternatives. The problem of indium migration into the active layers of organic electronics has caused researchers to look for alternative transparent electrodes without these drawbacks.¹⁰ Most importantly, because ITO has about 100 times lower conductivity than metals such as Ag and Al, thin metal films have recently been proposed for use as semi-transparent electrodes for photo-electronic devices with compromised transparency. Because of its monatomic thickness, graphene exhibits absolute transparency for a wide range of light frequencies.¹³ In addition, the excellent electric conductivity of graphene, as well as its chemical and mechanical stability, can be additional advantages as transparent electrode.

The band alignment at the interface between metal and semiconductor determines whether the contact is Ohmic or Schottky in type. Smaller interface energy barriers result in lower power consumption and higher conductance. In the present work, we investigate the features of graphene and their suitability for applications as electrode materials that interface directly with organic molecules. We show that the work function of graphene itself is not favorable for use as

anodes or cathodes of organic devices with conventional organic molecules. However, because of the chemical inertness of the sp^2 carbon surface, graphene has a particular advantage in the formation of charge-transfer complex with electron-accepting molecules.¹⁴ Despite electron transfer interactions with electron-accepting molecules, the graphene surface remains non-bonded, and the Fermi-level is well-aligned with the hole-injecting molecules.

For computations, we used the Vienna *Ab initio* Simulation Package (VASP) to calculate the ground state of many electrons system in the framework of density functional theory (DFT).^{15–18} A plane-wave basis set with an energy cut-off of 400 eV and Perdew-Burke-Ernzerhof (PBE)-type gradient-corrected exchange-correlation potential were employed.¹⁹ The ions were described by the projector augmented wave (PAW) potentials. All the atomic positions of graphene and adsorbate molecules were relaxed within residual forces smaller than 0.01 eV/Å.

Prior to modeling the interface between the graphene and the organic molecules, we investigated the work function of perfect graphene and thin metal layers. As model of thin metal layers, we chose four different types of metal slabs with thickness of three layers. Figures 1(a)–1(e) show the plane-averaged local potential plotted perpendicular to the surface (z -axis) of Pt(111), Au(111), graphene, Ag(111), and Ca(111), respectively. Here, the surfaces are in the xy plane. We placed a vacuum region about 10 Å along the perpendicular direction to the planes. As is typical, the work function is calculated by the energy difference between the Fermi level and the vacuum level which is the value of the flat potential at a far-separated region from the surface. Since the 2-D band structure of graphene has sharp linear dispersion around the K point (Dirac point), we controlled either the supercell size or the meshes for k -point sampling to include the Fermi point in the self-consistent field (SCF) procedure. Smearing width in the occupation factor near the Fermi level was tested

^{a)}Author to whom correspondence should be addressed. Electronic mail: noejung@unist.ac.kr.

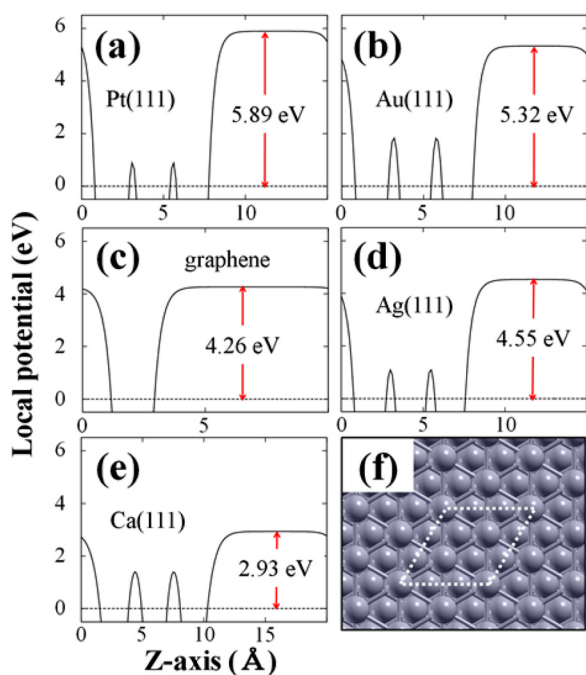


FIG. 1. The plane-averaged local potentials plotted along the perpendicular direction of thin metal surfaces. (a) Pt(111), (b) Au(111), (c) mono-layer graphene, (d) Ag(111), and (e) Ca(111) surfaces. (f) The dashed parallelogram indicates the computational unit cell of the (111) metal surfaces. The energies in the vertical axes are shown with respect to the Fermi level, which is indicated by dotted lines.

with 0.005 and 0.05 eV which resulted in almost the same result.

For efficient hole-injection, the anode surface is required to have a large work function. ITO has been severely oxidized to achieve such objective. On the other hand, inert noble metal (such as Pt or Au) can be deposited to increase the work function of the ITO surface.²⁰ For cathode electrode, a metal with a small work function is desired to achieve lower barrier for electron injection. Ca or alkaline can be selected as a cathode electrode. To characterize the feature of graphene, the work function of thin metals was calculated with the same computational scheme, as shown in Fig. 1. The overall result tells that, in terms of the work function, graphene is not suitable for use as the anodes or cathodes of typical organic devices. As shown in Fig. 1, the work function of graphene is about 1.3 (1.6) eV larger (smaller) than that of Ca (Pt). This magnitude of the work function is a critical demerit of graphene as an electrode, on either side of the anode and cathode, because it leads to a large Schottky barrier.

To more explicitly gauge whether graphene can replace conventional metal electrodes in organic electronic devices, we investigated the electronic structure at the interface between the graphene and typical hole-injection layers in the organic light-emitting diode (OLED). Cases with *N,N'*-Bis-(1-naphthalenyl)-*N,N'*-bis-phenyl-(1,1'-biphenyl)-4,4'-diamine (NPB) are shown in Figs. 2(a) and 2(b).^{21,22} As expected, the Fermi level of the graphene is 0.4 eV higher than the highest-occupied-molecular-orbital (HOMO) level of the NPB, as shown in Fig. 2(b). It is noteworthy that the Fermi level of the graphene is not well aligned with the HOMO of NPB, and therefore, a large Schottky barrier (in terms of hole

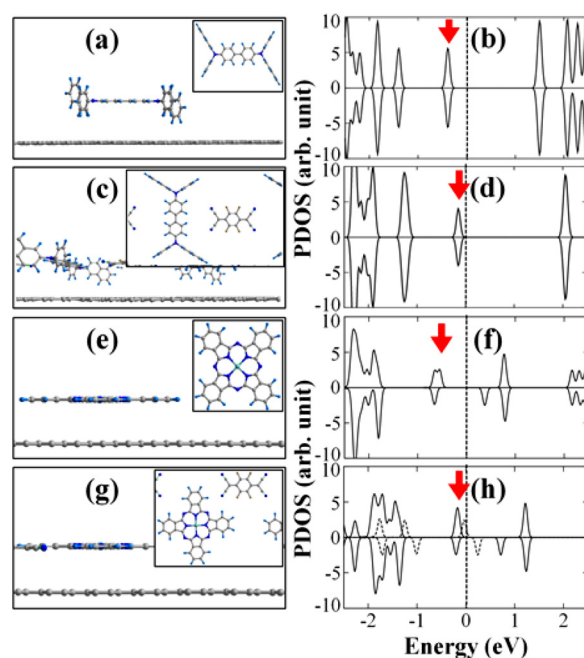


FIG. 2. (a) Side view of the NPB-adsorbed graphene and (b) the partial density of states (PDOS) for NPB. (c) Side view of the graphene with the adsorbed NPB and F4-TCNQ, and (d) PDOS of NPB. (e) Side view of the CuPc-adsorbed graphene, and (f) the PDOS for CuPc. (g) Side view of the graphene with the adsorbed CuPc and F4-TCNQ, and (h) the PDOS for CuPc (solid line) and F4-TCNQ (dotted line). In the insets of (a), (c), (e), and (g), the top views of molecules are shown while graphene is not shown for clarity. The downward arrows in (b), (d), (f), and (h) indicate the positions of the HOMO levels of NPB or CuPc.

injection) is expected between graphene and NPB if graphene is employed as an anode electrode for NPB.

Shallow co-evaporation of strong electron acceptors such as tetrafluoro-tetracyano-quinodimethane (F4-TCNQ) has been used to induce efficient hole injection at the anode interface.¹⁴ As an analogy, we investigated the electronic structure of graphene interfaced with the monolayer of NPB and F4-TCNQ, as shown in Fig. 2(c). Both molecules tend to self-arrange in a flat configuration on graphene, which is the most stable configuration on metal surfaces because more functional atoms of molecules interact with the surface atoms.²³ Unlike the case of NPB alone, we confirmed that the HOMO level of the NPB sits very close to the Fermi level of the graphene, as shown in Figs. 2(b) and 2(d). This energy level rearrangement is caused by the partial electron acceptance of F4-TCNQ from the graphene and the NPB. As a result, the Schottky barrier for hole injection from the graphene electrode to the NPB layer becomes negligible. If the nominal Schottky barrier is less than 0.2 eV at the metal-semiconductor interface, the contact-type can be considered as Ohmic near room temperature.²⁴

We performed similar studies of copper phthalocyanine (CuPc), as shown in Figs. 2(e)–2(h).^{25–27} In this case, the Fermi level of graphene is 0.6 eV higher than the HOMO level of CuPc, as shown in Figs. 2(e) and 2(f).²⁸ Similarly to the case of NPB, such a large mismatch between the Fermi levels of graphene with the HOMO level will lead to a large Schottky barrier between graphene and CuPc if graphene is employed as an anode material. The effect of the electron acceptor is more efficient in this case. With the presence of

F4-TCNQ, the HOMO level of CuPc becomes almost aligned with the Fermi level, as shown in Fig. 2(h). We note that the chemical inertness of graphene is an important component for the aforementioned band alignment. Even after the charge transfer from graphene to F4-TCNQ, they remain non-bonded only aligning the energy level. Such a strong electron transfer across the $\pi - \pi$ stacking distance (~ 3.4 Å) has also been widely observed in the pairs of F4-TCNQ and various other hole transport materials.²⁹ Below, we show that this advantage is due to the formation of charge-transfer complex and cannot be expected for the cases of metal surfaces with similar or smaller work functions.

For the cases of metal surface, the co-evaporation of electron-accepting molecular layers also reduced the hole-injection barrier.¹⁴ In such cases, electrostatic effect was dominant. After close examinations of the electronic structure, we found that the aforementioned energy level alignment cannot be simply attributed to electrostatic effect only. Instead, orbital coupling between graphene, F4-TCNQ, and CuPc (or NPB) is delicately involved. The co-adsorbed F4-TCNQ attracted electrons not only from CuPc but also from graphene, forming a type of charge-transfer complex.

We now show detailed electronic structures, as a result of spin-polarized calculations. Figures 3(a) and 3(b) show the electronic structure for the isolated CuPc and F4-TCNQ, which were calculated in large supercell with vacuum region being longer than 10 Å. One electron localized on the Cu site remained unpaired, as denoted by the upward arrow in Fig. 3(a). We calculated the electronic structure of the model geometry used for Fig. 2(g) only removing the graphene layer, as shown in Fig. 3(c). In this case, the charge transfer from CuPc to F4-TCNQ formed a charge transfer complex. Because of this electron transfer, the spin-up and the spin-down orbitals split, and one state of them sits on the Fermi level, as indicated by the down-ward arrow in Fig. 3(c). In the spin-polarized DFT results, when CuPc and F4-TCNQ formed independent co-planar structure without sub-layer, the spin directions of CuPc and F4-TCNQ are opposite, as shown Fig. 3(c), and the overall magnetization is found to be 0.45. However, when they are placed on the graphene plane,

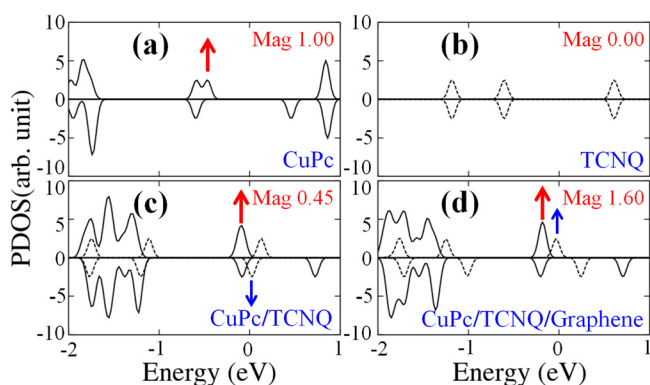


FIG. 3. Electronic structures of (a) CuPc and (b) F4-TCNQ in vacuum and (c) the layer of F4-TCNQ and CuPc without graphene layer and (d) with the graphene layer. The model geometry for (d) is the same as Fig. 2(g). Solid and dotted lines are for CuPc and F4-TCNQ, respectively. Upper and lower planes in (a)–(d) show the spin-up and spin-down states, respectively. Arrows indicate the non-paired orbitals which give rise to magnetic moment in the spin-polarized calculation. The numbers written as “Mag” denote the magnetization per unit cell.

the spin direction for both molecules is aligned parallel, as shown in Fig. 3(d). This clearly demonstrates that all three constituents (graphene, CuPc, F4-TCNQ) form a delicately involved charge-transfer complex. The features of exchange interaction, which is thought to be mediated by the graphene’s π electron and favors the aligned spins, required an independent in-depth study in view of organic magnetism.

To determine whether such co-evaporation is also effective on metal surfaces, we investigated the same co-evaporation on the Ag (111) surface, which has a work function similar to that of graphene, as shown in Fig. 1(d). As expected from the similarity of the work function, the HOMO of CuPc is about 0.36 eV below the Fermi level of the Ag (111) surface (Fig. 4(b)). This amount is likely to induce a substantial Schottky barrier at the interface between the Ag and the accumulated layer of CuPc. After co-evaporation of the CuPc and F4-TCNQ, the response of the Ag(111) surface is different from that of graphene. The four nitrogen terminals in the F4-TCNQ develop chemical bonds with the Ag atoms on the surface. Consequently, as shown in Fig. 4(c), the plane of the F4-TCNQ molecules bends toward the Ag(111) surface.

As a result, the HOMO level of CuPc remains distinct from the Fermi level of silver even with the presence of F4-TCNQ, as shown in Fig. 4(d). The electron-attracting feature of the F4-TCNQ largely disappears after forming a chemical bond with the Ag atoms. Therefore, the layer of F4-TCNQ is not effective for the alignment between the HOMO of CuPc and the Fermi level of silver. In previous paragraphs, we showed that the deposition of some electron acceptors on graphene makes it possible to modify the carrier injection barrier due to the presence of an interfacial dipole. But this work is diminished on the silver surface. The difference between graphene (Fig. 2) and Ag(111) (Fig. 4) is attributed to differences in chemical reactivities. In this type of application, the chemical inertness of graphene is an obvious advantage. In addition, such chemical inertness implies that the conductance of purified graphene can be robustly preserved against chemical perturbations.

In summary, using the first-principles computation methods, the interface between graphene and molecules of hole-injection layers in OLED (such as NPB or CuPc) was

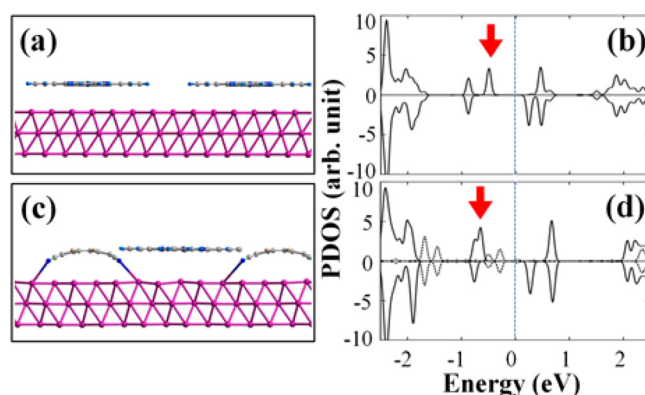


FIG. 4. (a) Side view of CuPc on the Ag(111) surface, and (b) the PDOS for CuPc molecules. (c) Side view of CuPc and F4-TCNQ molecules in contact with Ag(111) surface, and (d) the PDOS for CuPc (solid line) and F4-TCNQ (dotted line). The downward arrows in (b) and (d) indicate the positions of the HOMO level of CuPc.

investigated. We showed that the chemical inertness of the graphene surface is a good advantage of graphene as an electrode. After a trace of charge transfer to the electron-accepting molecule (F4-TCNQ), the Fermi level of graphene is well aligned with the HOMO of the hole-injection molecules (NPB or CuPc). This is a unique merit of the sp^2 -bonded carbon, which is absent in thin metal layers. We suggest that a proper choice of charge transfer complex can decently tune energy level of organic molecules with the graphene Fermi level.

This work was supported by the 2011 Research Fund of the UNIST. N.P. and H.J. were supported by the National Research Foundation of Korea funded by the Ministry of Education, Science, and Technology (MEST) (Grant No. 2009-0087731). G.B. and W.P. were supported by the Basic Science Research Program (No. 2011-0006268). S.H. and J.P. were supported by Priority Research Centers Program (No. 2011-0018395) and the Converging Research Center Program (No. 2011K000620).

- ¹K. S. Novoselov, A. K. Geim, S. V. Morozov, D. Jiang, Y. Zhang, S. V. Dubonos, I. V. Grigorieva, and A. A. Firsov, *Science* **306**, 666 (2004).
- ²K. S. Novoselov, A. K. Geim, S. V. Morozov, D. Jiang, M. I. Katsnelson, I. V. Grigorieva, S. V. Dubonos, and A. A. Firsov, *Nature* **438**, 197 (2005).
- ³Y. Zhang, Y.-W. Tan, H. L. Stormer, and P. Kim, *Nature* **438**, 201 (2005).
- ⁴S. Sachdev and M. Muller, *J. Phys.: Condens. Matter* **21**, 164216 (2009).
- ⁵S. Stankovich, D. A. Dikin, G. H. B. Dommett, K. M. Kohlhaas, E. J. Zimmerman, E. A. Stach, R. D. Piner, S. T. Nguyen, and R. S. Ruoff, *Nature (London)* **442**, 282 (2006).
- ⁶N. Mohanty and V. Berry, *Nano Lett.* **8**, 4469 (2008).
- ⁷M. D. Stoller, S. Park, Y. Zhu, J. An, and R. S. Ruoff, *Nano Lett.* **8**, 3498 (2008).

- ⁸B. N. Szafraneck, D. Schall, M. Otto, D. Neumaier, and H. Kurz, *Appl. Phys. Lett.* **96**, 112103 (2010).
- ⁹Y. Q. Wu, P. D. Ye, M. A. Capano, Y. Xuan, Y. Sui, M. Qi, J. A. Cooper, T. Shen, D. Pandey, G. Prakash, and R. Reifengerger, *Appl. Phys. Lett.* **92**, 092102 (2008).
- ¹⁰J. Wu, M. Agrawal, H. A. Becerril, Z. Bao, Z. Liu, Y. Chen, and P. Peumans, *ACS Nano* **4**, 43 (2010).
- ¹¹S. Bae, H. Kim, Y. Lee, X. Xu, J.-S. Park, Y. Zheng, J. Balakrishnan, T. Lei, H. R. Kim, Y. I. Song, Y.-J. Kim, K. S. Kim, B. Ozyilmaz, J.-H. Ahn, B. H. Hong, and S. Iijima, *Nat. Nanotechnol.* **5**, 574 (2010).
- ¹²K. S. Kim, Y. Zhao, H. Jang, S. Y. Lee, J. M. Kim, K. S. Kim, J.-H. Ahn, P. Kim, J.-Y. Choi, and B. H. Hong, *Nature* **457**, 706 (2009).
- ¹³X. Wang, L. Zhi, and K. Mullen, *Nano Lett.* **8**, 323 (2008).
- ¹⁴N. Koch, S. Duhm, J. P. Rabe, A. Vollmer, and R. L. Johnson, *Phys. Rev. Lett.* **95**, 237601 (2005).
- ¹⁵B. Hohenberg and W. Kohn, *Phys. Rev.* **136**, B864 (1964).
- ¹⁶W. Kohn and L. J. Sham, *Phys. Rev.* **140**, A1133 (1965).
- ¹⁷G. Kresse and J. Furthmuller, *Phys. Rev. B* **54**, 11169 (1996).
- ¹⁸G. Kresse and J. Furthmuller, *Comput. Mater. Sci.* **6**, 15 (1996).
- ¹⁹J. P. Perdew, K. Burke, and M. Ernzerhof, *Phys. Rev. Lett.* **77**, 3865 (1996).
- ²⁰S. M. Tadayyon, K. Griffiths, P. R. Norton, C. Tripp, and Z. Popovic, *J. Vac. Sci. Technol. A* **17**, 1773 (1999).
- ²¹M. Dong, X. Wu, Y. Hua, Q. Qi, and S. Yin, *Chin. Phys. Lett.* **27**, 127802 (2010).
- ²²T. Sun, Z. L. Wang, Z. J. Shi, G. Z. Ran, W. J. Xu, Z. Y. Wang, Y. Z. Li, L. Dai, and G. G. Qin, *Appl. Phys. Lett.* **96**, 133301 (2010).
- ²³X. Tian, J. Xu, and X. Wang, *J. Phys. Chem. B* **114**, 11377 (2010).
- ²⁴M. Murakami and Y. Koide, *Crit. Rev. Solid State Mater. Sci.* **23**, 1 (1998).
- ²⁵S. M. Tadayyon, H. M. Grandin, K. Griffiths, P. R. Norton, H. Aziz, and Z. D. Popovic, *Org. Electron.* **5**, 157 (2004).
- ²⁶T. H. Lee, K. M. Lai, and L. M. Leung, *Polymer* **50**, 4602 (2009).
- ²⁷Y. Wang, J. Ren, C. Song, Y. Jiang, L. Wang, K. He, X. Chen, J. Jia, S. Meng, E. Kaxiras, Q. Xue, and X.-C. Ma, *Phys. Rev. B* **82**, 245420 (2010).
- ²⁸J. Ren, S. Meng, Y. Wang, X. Ma, Q. Xue, and E. Kaxiras, *J. Chem. Phys.* **134**, 194706 (2011).
- ²⁹L. Zhu, E.-G. Kim, Y. Yi, and J.-L. Brédas *Chem. Mater.* **23**, 5149 (2011).